

# Generalized parton distributions of pseudoscalar mesons in a covariant constituent quark model

A. Van Dyck<sup>1</sup>, T. Van Cauteren<sup>1a</sup>, J. Ryckebusch<sup>1</sup>, and B. C. Metsch<sup>2</sup>

<sup>1</sup> Department of Subatomic and Radiation Physics, Ghent University, Proeftuinstraat 86, B-9000 Gent, Belgium

<sup>2</sup> Helmholtz-Institut für Strahlen- und Kernphysik, Nußallee 14-16, D-53115 Bonn, Germany

Received: date / Revised version: date

**Abstract.** The isoscalar twist-two generalized parton distributions (GPDs) of the pion and the kaon are calculated in a Poincaré covariant Bethe-Salpeter constituent quark model. Results are presented for several values of the parameters  $\xi$  and  $t$ . The results satisfy the form factor constraints and the polynomiality condition. For the pion GPD, also the isospin symmetry constraint is fulfilled. The influence of kinematical variables and model parameters on the support of the GPDs is investigated. To this end, the strength parameters and quark masses of the constituent quark model are artificially varied.

**PACS.** 11.10.St Bound and unstable states; Bethe-Salpeter equations – 12.39.Ki Relativistic quark model – 13.60.Fz Elastic and Compton scattering – 14.40.Aq  $\pi$ ,  $K$  and  $\eta$  mesons

## 1 Introduction

Unraveling the substructure of hadrons is a challenging issue. Whereas the theory of QCD provides us with the equations governing the quark-gluon dynamics, the exact way in which they form colorless bound states in the non-perturbative regime remains elusive to date. It is expected that the endeavor of measuring and computing generalized parton distribution functions (GPDs) will contribute significantly to a full description of hadron structure [1]. GPDs are a natural unification of form factors (FFs) and parton distribution functions (PDFs) within one framework. They describe the non-perturbative part of the deeply virtual Compton scattering (DVCS) and hard exclusive meson production (HEMP) processes.

A calculation of GPDs from first QCD principles is beyond reach at this moment. Therefore, numerous model calculations have been presented in the last years [2, 3, 4, 5, 6, 7, 8, 9, 10]. In this work, we present results for the pion and kaon GPDs computed within the framework of the Bethe-Salpeter model developed in refs. [11, 12, 13, 14]. The pseudoscalar ground-state mesons have a simple valence-quark substructure and possess only one helicity-conserving GPD, which makes the calculation less cumbersome than for nucleons. Yet, such a calculation provides insight in the dependence of the GPDs on hadron structure in the non-perturbative regime.

In order to compare the GPDs computed in a phenomenological model with the data from deeply inelastic scattering experiments, a  $Q^2$ -evolution needs to be performed [15]. The evolution equations depend highly

on the kinematic region of the process. More specifically, one can distinguish between the DGLAP and ERBL regions, where the  $Q^2$ -evolution is governed by the DGLAP and the ERBL equations, respectively. Parton model constraints make GPDs vanish outside these two regions [16, 17]. A model which resolves the ERBL and the DGLAP regions and has a vanishing GPD otherwise, is said to have the correct support.

In ref. [18] we have demonstrated that a support problem may arise in dynamic quark models based on the BS approach if the interaction depends on the minus component of the relative momentum between the constituent quark and antiquark. Note that this condition is necessary but not sufficient and that a support problem does not necessarily arise when the interaction depends on the minus component of the relative momentum. Furthermore, we provided representative results computed within the explicitly Poincaré covariant constituent quark model developed by the Bonn group [11], where a support problem did arise.

In this work, we focus on the influence of the meson binding energy on the support. The pion and the kaon are ideal for such a study because the former is a very deeply and the latter a moderately deeply bound state of quark and antiquark. Both the absolute binding energy and meson mass are altered by changing the input quark masses and effective interaction strength. Yet the degree of support violation depends mostly on the relative binding energy. Results will be shown for the isoscalar twist-two quark GPD of the pion and the kaon at different relative binding energies and for different values of

<sup>a</sup> e-mail: Tim.VanCauteren@UGent.be

the squared fourmomentum transfer  $t$  and relative plus-momentum transfer  $\xi$ .

This paper is organized as follows. Section 2 presents the definition of the GPD and the relevant kinematics. The Bonn model is introduced in sect. 3, while sect. 4 is devoted to the calculation of GPDs in this model. In this section, we will also introduce the three model variants which will be used in sect. 5. There, we show our results for the pion GPD. A summary and an outlook to future research are given in sect. 6.

## 2 Definition and Conventions

GPDs are non-diagonal matrix elements of a bilocal field operator on the light cone. For partons with spin 1/2 in a pseudoscalar meson, the GPD associated with helicity conserving partons is defined as follows [16]:

$$H^f(x, \xi, t) = \frac{1}{2} \int \frac{dz^-}{2\pi} e^{ix\bar{P}^+z^-} \langle \bar{P}' | \bar{\psi}^f(-\frac{z}{2}) \gamma^+ \psi^f(\frac{z}{2}) | \bar{P} \rangle \Big|_{z^+=0, \mathbf{z}_\perp=0}. \quad (1)$$

In this equation,  $f$  refers to the flavor of the probed parton, while  $\bar{P} = \frac{\bar{P}'+\bar{P}}{2}$  and  $t = \Delta^2 = (\bar{P}' - \bar{P})^2$ . Definition (1) uses light-cone coordinates. A fourmomentum  $p = (p^0, p^1, p^2, p^3)$  can be written in light-cone coordinates as  $p = [p^+, p^-, \mathbf{p}_\perp]$  with  $p^\pm = (p^0 \pm p^3)/\sqrt{2}$  and  $\mathbf{p}_\perp = (p^1, p^2)$ . The skewedness  $\xi$  and the average plus-momentum fraction of the struck parton  $x$  are defined in fig. 1:  $x$  denotes the fraction of the average meson plus-momentum that is reabsorbed by the meson, while  $\xi$  is a measure for the plus-momentum that is lost in the process:

$$\xi = \frac{\bar{P}^+ - \bar{P}'^+}{\bar{P}^+ + \bar{P}'^+}. \quad (2)$$

These definitions coincide with the symmetrical variables that were introduced by Ji [19]. Their interpretation as plus-momentum fractions holds in the infinite momentum frame. In literature, another set of variables  $(X, \zeta)$  has been introduced by Radyushkin [20], with  $X = \frac{(x+\xi)}{(1+\xi)}$  and  $\zeta = \frac{2\xi}{(1+\xi)}$ . Although Radyushkin's variables are more closely related to the ones used in forward kinematics, we will use Ji's choice of variables, as they reflect the symmetry between the incoming and outgoing hadron states.

Definition (1) is valid when the partons do not transfer helicity. It only holds in a coordinate system where  $\mathbf{q}$  and  $\bar{\mathbf{P}}$  are collinear and in the three-direction [21]. From definition (1), it is clear that the GPDs are Lorentz invariant quantities. This means that, although they are defined on the light cone, the GPDs can be calculated in any convenient reference frame, provided that the average transverse hadron momentum  $\bar{\mathbf{P}}_\perp = \mathbf{0}$ . Whenever a specific choice is needed, we will choose a Breit frame which matches these conditions.

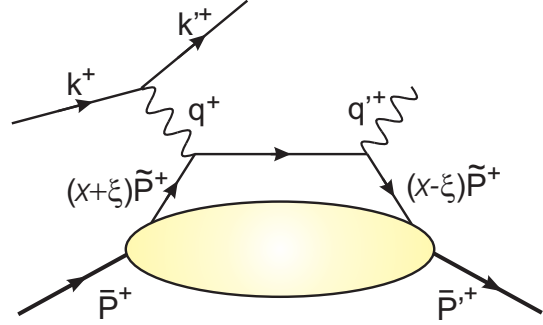


**Fig. 1.** The Feynman diagram of DVCS on the light cone, with the definition of the kinematical variables  $x$  and  $\xi$ .

The skewedness  $\xi$  is restricted to the interval  $[0, \xi_{max}]$  with

$$\xi_{max} = \sqrt{\frac{-t}{4M^2 - t}}, \quad (3)$$

where  $M$  is the hadron mass.

Stringent tests for any model calculation are found in the following GPD properties. The first is the relation between the electromagnetic form factor and the GPD,

$$\int dx H^f(x, \xi, t) = F^f(t), \quad (4)$$

where  $\xi$  factors out and the partial electromagnetic form factors  $F^f$  are defined through

$$F = \sum_f e_f F^f, \quad (5)$$

with  $e_f$  the electric charge of a parton with flavor  $f$ . The second model constraint is called the polynomiality condition, which states that the  $n$ th Mellin moment of the GPD is a polynomial in  $\xi$  of order  $\leq n$  [21]:

$$\int dx x^{n-1} H^f(x, \xi, t) = \sum_{i=0}^n a_i(t) \xi^i, \quad (6)$$

where the coefficients  $a_i$  of the polynomial depend on  $t$ . The polynomiality condition can be regarded as a more general form of the above form factor relation. Finally, for pions, isospin invariance and charge conjugation lead to the following relation:

$$H_\pi^q(x, \xi, t) = -H_\pi^{\bar{q}}(-x, \xi, t). \quad (7)$$

We will come back to these model constraints in sect. 5.

## 3 Formalism

In the Bonn model, mesons are described as bound states of a constituent quark and antiquark. The model, based on the Bethe-Salpeter equation, is Poincaré covariant by construction. Explicit covariance is important in the calculation of the GPD of pseudoscalar mesons for two reasons. First, the pion is a “deeply-bound” boson whose

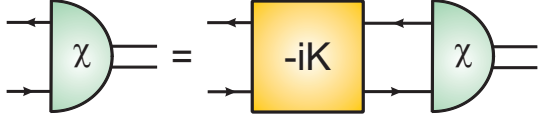


**Fig. 2.** Diagrammatic representation of the Bethe-Salpeter equation (9).

static and dynamic properties are best reproduced with a relativistic model [22]. Second, in the calculation of dynamic quantities such as the GPD, recoil fourmomenta have to be treated relativistically. The Bonn model is a few-parameter model with only seven parameters which are fitted to the meson mass spectrum [11]. The fact that no relativistic corrections need to be implemented is an enormous asset to minimize the amount of parameters and maximize the predictive power. In refs. [11, 12, 13, 14], the Bonn model is described in detail. In sects. 3.1 and 3.2, we give a brief summary to make this paper more self-contained.

### 3.1 The model ingredients

A meson with on-shell fourmomentum  $\bar{P}$  is described by the Bethe-Salpeter amplitude

$$\chi_{\bar{P}\alpha\beta}(x_1, x_2) = \langle \Theta | T \{ \psi_\alpha^1(x_1) \bar{\psi}_\beta^2(x_2) \} | \bar{P} \rangle, \quad (8)$$

where  $T$  is the time ordering operator acting on the Heisenberg fermion field operators  $\psi_\alpha$ . The indices in Dirac, flavor and color space are combined in the multi-indices  $\alpha \equiv (\alpha, f, c)$ . The variables  $x_1$  and  $x_2$  are the fourvectors denoting the spacetime positions of the quark and the antiquark, respectively.

The Bethe-Salpeter amplitude (8) is the solution of the Bethe-Salpeter equation, which in momentum space reads [12, 23]:

$$\chi_{\bar{P}} = -iG_{0\bar{P}}K_{\bar{P}}\chi_{\bar{P}}. \quad (9)$$

Here, indices and arguments have been suppressed for notational simplicity. It is tacitly assumed that one integrates over arguments and sums over indices that occur twice.  $G_{0\bar{P}}$  is the product of the one-particle propagators, while  $K_{\bar{P}}$  denotes the interaction kernel. The pictorial representation of eq. (9) is shown in fig. 2. The normalization of the Bethe-Salpeter amplitudes is given by [12]:

$$\bar{\chi}_{\bar{P}} \left[ P^\mu \frac{\partial}{\partial P^\mu} (G_{0\bar{P}}^{-1} + iK_{\bar{P}}) \right]_{P=\bar{P}} \chi_{\bar{P}} = 2iM^2. \quad (10)$$

Note that eq. (10) is written in a frame independent way.

To transform the Bethe-Salpeter equation (9) into a solvable integral equation, two *Ansätze* are made. The first assumption is the instantaneous approximation of the interaction kernel  $K_{\bar{P}}$ ,

$$K_{\bar{P}}(p, p') \equiv V(p_{\perp\bar{P}}, p'_{\perp\bar{P}}), \quad (11)$$

where  $p_{\perp P} \equiv p - (p \cdot P/P^2)P$  is the fourvector perpendicular to  $P$  with  $p$  the relative fourmomentum between

the constituent quark and the constituent antiquark in the meson. Within the instantaneous approximation, all retardation effects are neglected. Strictly speaking, this is justified for a part of the interaction (*e.g.* the (colour-)Coulomb-interaction) in a specific gauge (*e.g.* the Coulomb gauge) only. Otherwise this approximation will lead to a non-local and non-causal model. Nevertheless, the model equations lead to frame-independent results. Hence, the model can be called Poincaré covariant. The second assumption is that the full quark propagators  $S_j^F(p)$  can suitably be approximated by free fermion propagators with an effective constituent quark mass  $m_j$ ,

$$S_j^F(p) \equiv \frac{i}{\not{p} - m_j + i\epsilon}. \quad (12)$$

The constituent quark masses are model parameters. Because isospin symmetry is exact in the Bonn model, the calculation of the low-lying meson spectrum requires only two mass parameters: the non-strange and the strange quark mass.

### 3.2 Reduction to the Salpeter equation

The Salpeter amplitude  $\Phi(\mathbf{p})$  in the rest frame of the bound state is defined as follows:

$$\Phi(\mathbf{p}) = \int \frac{d^4p^0}{2\pi} \chi_{\bar{P}}(p^0, \mathbf{p}) |_{\bar{P}=(M, \mathbf{0})}. \quad (13)$$

Making use of eqs. (11) and (13), the  $p^0$ -integration in eq. (9) can be carried out, leading to the well-known Salpeter equation [24]:

$$\begin{aligned} \Phi(\mathbf{p}) = & \int \frac{d^3p'}{(2\pi)^3} \frac{\Lambda_1^-(\mathbf{p})\gamma^0[V(\mathbf{p}, \mathbf{p}')\Phi(\mathbf{p}')]\gamma^0\Lambda_2^+(-\mathbf{p})}{M + \omega_1 + \omega_2} \\ & - \int \frac{d^3p'}{(2\pi)^3} \frac{\Lambda_1^+(\mathbf{p})\gamma^0[V(\mathbf{p}, \mathbf{p}')\Phi(\mathbf{p}')]\gamma^0\Lambda_2^-(-\mathbf{p})}{M - \omega_1 - \omega_2}, \end{aligned} \quad (14)$$

with the energy projection operators  $\Lambda_j^\pm = (\omega_j \pm H_j)/(2\omega_j)$ , the Dirac Hamiltonian  $H_j(\mathbf{p}) = \gamma^0(\boldsymbol{\gamma} \cdot \mathbf{p} + m_j)$  and the energy  $\omega_j = \sqrt{m_j^2 + |\mathbf{p}|^2}$  for the  $j$ th constituent quark.

The potentials used in our calculations are the *confinement interaction*  $\mathcal{V}$  and the *'t Hooft instanton induced interaction*  $V_{III}$  [25]. The confinement potential rises linearly with the interquark distance and is multiplied by a Dirac structure which reproduces the observed mass splittings in the meson spectrum [26, 27]:

$$\begin{aligned} \mathcal{V}(|\mathbf{x}_q - \mathbf{x}_{\bar{q}}|) = & \frac{1}{2}(a_c + b_c|\mathbf{x}_q - \mathbf{x}_{\bar{q}}|) \\ & \times (\mathbf{1} \otimes \mathbf{1} - \boldsymbol{\gamma}^5 \otimes \boldsymbol{\gamma}^5 - \boldsymbol{\gamma}_\mu \otimes \boldsymbol{\gamma}^\mu), \end{aligned} \quad (15)$$

where  $\mathbf{x}_{q(\bar{q})}$  is the position of the constituent (anti-)quark. The instanton interaction accounts for the mass splittings

in the pseudoscalar and the scalar sectors [22]. In momentum space, it can be written as

$$\int \frac{d^3 p'}{(2\pi)^3} V_{III}(\mathbf{p}, \mathbf{p}') \Phi(\mathbf{p}') = 4G(g, g') \times \int \frac{d^3 p'}{(2\pi)^3} \mathcal{R}_\Lambda(\mathbf{p}, \mathbf{p}') (\mathbb{1} \text{Tr}[\Phi(\mathbf{p}')] + \gamma^5 \text{Tr}[\gamma^5 \Phi(\mathbf{p}')] ), \quad (16)$$

where  $G(g, g')$  includes the flavor dependent couplings  $g$  and  $g'$ , and  $\mathcal{R}_\Lambda$  is a Gaussian regulating function with cut-off  $\Lambda$  [26, 27]. The 't Hooft instanton induced interaction can account for the low mass of the pion. The confinement and the instanton interaction contain five additional model parameters, bringing the total to seven. These seven model parameters are fitted to the Regge trajectories and the pseudoscalar ground state masses and are kept fixed in the calculation of dynamic observables. In this sense, the results in sect. 5 are predictions.

The Salpeter amplitudes  $\Phi$  are calculated by solving eq. (14). Imposing the normalization condition, written in terms of the Salpeter amplitudes, then yields the mass spectrum [12].

## 4 GPDs in the Bethe-Salpeter Quark Model

The first step in the calculation of the generalized parton distribution defined by eq. (1) is the calculation of the bilocal current matrix element  $\langle \bar{P}' | \bar{\psi}(-\frac{z}{2}) \gamma^+ \psi(\frac{z}{2}) | \bar{P} \rangle$ . In a Bethe-Salpeter based approach, the matrix element of any dynamic variable can be calculated with the Mandelstam formalism [28]. This formalism acts as a starting point for the derivation of the GPD in terms of the Bethe-Salpeter amplitudes. A straightforward calculation yields the bilocal current matrix element in lowest order [27]:

$$\begin{aligned} & \langle \bar{P}' | \bar{\psi}(-\frac{z}{2}) \gamma^+ \psi(\frac{z}{2}) | \bar{P} \rangle \\ &= \int d^4 x'_2 i \text{Tr} \left\{ \bar{\chi}_{\bar{P}'}(x'_2, \frac{z}{2}) \left( (i \not{\partial}_{x'_2} - m_1) \chi_{\bar{P}}(x'_2, -\frac{z}{2}) \right) \gamma^+ \right\} \\ &+ \int d^4 y'_1 i \text{Tr} \left\{ \left( (i \not{\partial}_{y'_1} - m_2) \bar{\chi}_{\bar{P}'}(-\frac{z}{2}, y'_1) \right) \gamma^+ \chi_{\bar{P}}(\frac{z}{2}, y'_1) \right\}. \end{aligned} \quad (17)$$

The second term in eq. (17) (coupling to the quark) is depicted in fig. 3. Inserting eq. (17) in eq. (1) gives

$$H(x, \xi, t) = H^q(x, \xi, t) + H^{\bar{q}}(x, \xi, t), \quad (18)$$

with the term originating from the quark-current coupling,

$$\begin{aligned} H^q(x, \xi, t) &= \frac{i}{2} \int \frac{d^4 p}{(2\pi)^4} \delta \left( x \tilde{P}^+ - \frac{\bar{P}'^+}{2} - p^+ \right) \\ &\times \text{Tr} \left\{ \left( -\frac{\bar{P}}{2} + \not{p} - m_2 \right) \bar{\chi}_{\bar{P}'}(p + \frac{\bar{P}'}{2} - \frac{\bar{P}}{2}) \gamma^+ \chi_{\bar{P}}(p) \right\}, \end{aligned} \quad (19)$$

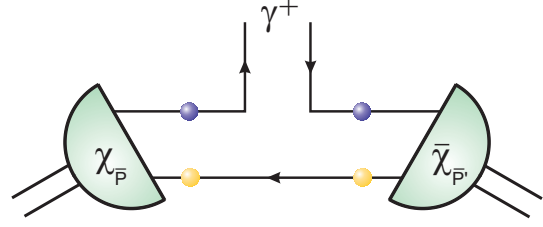


**Fig. 3.** Schematic representation of the second term in expression (17) for the plus-component of the bilocal current matrix element.

and the term originating from the antiquark-current coupling,

$$\begin{aligned} H^{\bar{q}}(x, \xi, t) &= \frac{i}{2} \int \frac{d^4 p}{(2\pi)^4} \delta \left( x \tilde{P}^+ + \frac{\bar{P}'^+}{2} - p^+ \right) \\ &\times \text{Tr} \left\{ \bar{\chi}_{\bar{P}'}(p + \frac{\bar{P}}{2} - \frac{\bar{P}'}{2}) \left( \frac{\bar{P}}{2} + \not{p} - m_1 \right) \chi_{\bar{P}}(p) \gamma^+ \right\}. \end{aligned} \quad (20)$$

Equations (17)-(20) make use of the full Bethe-Salpeter amplitude  $\chi$ . This amplitude can be reconstructed from the Salpeter amplitudes as follows: once the Salpeter equation is solved, the vertex functions  $\Gamma_{\bar{P}} = G_{0\bar{P}}^{-1} \chi_{\bar{P}}$  can be calculated. In the meson rest frame, these vertex functions read:

$$\Gamma_{\bar{P}}(p_{\perp} \bar{P}) |_{\bar{P}=(M,0)} = \Gamma(p) = -i \int \frac{d^3 p}{(2\pi)^3} [V(p, p') \Phi(p')]. \quad (21)$$

By Lorentz boosting the resulting Bethe-Salpeter amplitude from the meson rest frame to the frame in which the meson has on-shell momentum  $\bar{P}$ , the amplitude in the latter frame is found:

$$\chi_{\bar{P}}(p) = S_{A_{\bar{P}}} \chi_{(M,0)}(A_{\bar{P}}^{-1} p) S_{A_{\bar{P}}}^{-1}. \quad (22)$$

In this equation,  $A_{\bar{P}}$  denotes the Lorentz transformation and  $S_{A_{\bar{P}}}$  denotes the corresponding boost operator acting on the fermion field operators in eq. (9). Due to the instantaneous approximation, the boost properties of the Bethe-Salpeter amplitude are described by the above equation. All interaction dependence effectively enters the boost operator through the bound state's mass.

Written in terms of these vertex functions, the quark GPD arising from the Mandelstam formalism contains three quark propagators  $S_F$ :

$$\begin{aligned} H_\pi^q(x, \xi, t) &= -\frac{1}{2} \int \frac{d^4 p}{(2\pi)^4} \delta \left( \frac{2x + \xi - 1}{2(1 + \xi)} \bar{P}^+ - p^+ \right) \\ &\times \text{Tr} \left\{ \bar{\Gamma}_{\bar{P}'}(p + \frac{\Delta}{2}) S_F^1(\frac{\bar{P}'}{2} + p + \frac{\Delta}{2}) \gamma^+ \right. \\ &\quad \left. S_F^1(\frac{\bar{P}}{2} + p) \Gamma_{\bar{P}}(p) S_F^2(-\frac{\bar{P}}{2} + p) \right\}, \end{aligned} \quad (23)$$

These propagators can be directly linked with the intermediate quark lines in the diagram of fig. 3. It turns out

Parameter	Full model	Reduced model	IQM model
$m_n$ [MeV]	380	380	800
$m_s$ [MeV]	550	550	-
$a_c$ [MeV]	-1135	-1135	-1135
$b_c$ [MeV/fm]	1300	1300	1300
$g$ [GeV <sup>-2</sup> ]	1.62	0.0	1.62
$g'$ [GeV <sup>-2</sup> ]	1.35	0.0	1.35
$\Lambda$ [fm]	0.42	-	0.42
$M_\pi$ [MeV]	141	572	1095
$\Delta_M^\pi$ [MeV]	619	188	505
$\Delta_M^\pi/M_\pi$	4.39	0.33	0.46
$M_K$ [MeV]	506	728	-
$\Delta_M^K$ [MeV]	424	202	-
$\Delta_M^K/M_K$	0.84	0.28	-

**Table 1.** Overview of the parameters of the three models that were used in this work: the constituent quark masses, the confinement offset and slope, the 't Hooft interaction range and the 't Hooft interaction strengths. Also presented is a summary of the masses  $M$ , binding energies  $\Delta_M$  and relative binding energies  $\Delta_M/M$  of the pion and the kaon in the different models.

that the denominators of these three propagator terms ensure the correct support region for the GPDs,  $x \in [-\xi, 1]$  (ERBL and DGLAP regions) for  $p^-$  independent vertex functions. For  $p^-$  dependent vertex functions, it is a priori unclear whether the GPD will be confined to the support region. In previous work, we have shown that the Bonn model is prone to a support problem [18]. In the next paragraphs, we will quantitatively investigate which physical parameters influence the support behavior of the model. The role of the variables  $\xi$  and  $t$  will be analyzed, and the dependence on the binding strength will be examined through a comparison of the GPD of the kaon and the pion in three different model variants.

#### 4.1 Model variants

In the forthcoming section, the GPDs of pseudoscalar mesons will be shown in three different model variants: the full model, the reduced model and the increased quark mass (IQM) model. The parameters of these models are presented in table 1. Notice that the parameters  $a_c$  and  $b_c$  of the confinement interaction remain fixed for all three model variants.

##### 4.1.1 Full model

The full model is the one referred to as Model  $\mathcal{B}$  in ref. [26]. It provides an accurate description of the pion and other meson properties such as its mass, electromagnetic form factor, electroweak decay widths, etc. In the full model, the pion mass is calculated as  $M_\pi^{full} = 141$  MeV which implies a large mass defect of  $\Delta_{M_\pi}^{full} = (2m_n - M_\pi^{full}) = 619$  MeV; accordingly we shall call the pion

“deeply bound”. The kaon is moderately bound in this model, with a mass of  $M_K^{full} = 506$  MeV and a mass defect of  $\Delta_{M_K}^{full} = (m_n + m_s - M_K^{full}) = 424$  MeV.

##### 4.1.2 Reduced model

In the reduced model, the 't Hooft instanton induced interaction is omitted. As we have mentioned in sect. 3.2, the instanton interaction accounts for the deep binding of the pion (and to a lesser degree also of the kaon). Accordingly, neglecting the 't Hooft interaction will provide insight into the importance of binding effects in the GPD results. As a matter of fact, the calculated pion mass increases to  $M_\pi^{red} = 572$  MeV in this approach ( $\Delta_{M_\pi}^{red} = 188$  MeV). The kaon mass increases to  $M_K^{red} = 728$  MeV ( $\Delta_{M_K}^{red} = 202$  MeV).

##### 4.1.3 Increased quark mass (IQM) model

Not only the 't Hooft instanton induced interaction has an effect on the pion binding energy. Also the non-strange constituent quark mass  $m_n$  affects the pion mass and mass defect. To investigate the influence of the binding energy on the support of the generalized parton distributions, both mechanisms must be studied.

In the IQM model, we will only show results for the pion GPD. After combining the IQM model results with the kaon results from the full model, one can determine the influence of the heavy quarks. Increasing the non-strange quark mass by more than a factor of 2 to  $m_n = 800$  MeV yields a pion mass of  $M_\pi^{IQM} = 1095$  MeV. The mass defect in this model is  $\Delta_{M_\pi}^{IQM} = 505$  MeV.

##### 4.1.4 Model summary

The masses, binding energies and relative binding energies (defined as the binding energy divided by the mass) calculated in the different models are summarized in table 1. The deep binding of the pion in the full model is reflected in the high relative binding energy.  $\Delta_M/M$  in the full model is much smaller for the kaon than for the pion. Further,  $\Delta_M/M$  of the kaon in the full model is larger than in the reduced model, and also larger than  $\Delta_M/M$  of the pion in the reduced and the IQM models. In sect. 5, we will come back to these (relative) binding energies.

#### 4.2 Model constraints

In sect. 2, we introduced three constraints that serve as stringent tests for any GPD calculation. These are the isospin symmetry relation (7) for the pion GPD, the form factor relation (4) and the polynomiality condition (6). In this section, we elaborate on these constraints, and show that they are fulfilled in our model.

The pion up and down quark GPDs must fulfill the isospin symmetry relation of eq. (7). The equality is exact in our calculations. The strange quark content of the kaon prevents an isospin symmetry relation of the type (7).written. The results show a small difference between the quark and antiquark GPDs at opposite  $x$  (*e.g.* in the full model,  $H_{K^+}^u(x=0.5, \xi=0, t=-0.5 \text{ GeV}^2) = 0.764$  versus  $H_{K^+}^s(x=-0.5, \xi=0, t=-0.5 \text{ GeV}^2) = -0.784$ ). We will elaborate on these differences in sect. 5.

The GPD is related to the electromagnetic form factor through relation (4). Taking into account eq. (5), which relates the partial form factors with the meson form factor, and the isospin symmetry relation (7) for the pion, one finds that

$$\int_{-\infty}^{+\infty} dx H_{\pi^+}^u(x, \xi, t) = F_{\pi^+}(t). \quad (24)$$

Note that, due to the support properties of the GPDs in the Bonn model, the integration domain is  $x \in (-\infty, +\infty)$ . For the kaon, the relation becomes

$$e_u \int_{-\infty}^{+\infty} dx H_{K^+}^u(x, \xi, t) + e_s \int_{-\infty}^{+\infty} dx H_{K^+}^s(x, \xi, t) = F_{K^+}(t), \quad (25)$$

where  $e_u = 2/3$  and  $e_s = -1/3$ .

We have compared the results of eqs. (24) and (25) with a direct computation of the electromagnetic form factors  $F_{\pi^+}$  and  $F_{K^+}$  in the Bonn model [11]. These numerical calculations were performed independently and yielded results which were compatible at the few-% level [27]. When discussing these form factors results, it is worth stressing that the instantaneous approximation does not result in current non-conservation. Although the EM current in lowest order in the instantaneous approximation generally does not fulfill the Ward-Takahashi identity, it does so in the case of a  $0^- \rightarrow 0^-$  elastic matrix element [14].

An even more stringent test than the form-factor condition of eq. (4), is the polynomiality condition of eq. (6). This condition was verified numerically for different values of  $t$  up to order  $n = 5$  [27].

In [29], the authors point out that the parton distribution (PD) of the pion should fulfill four conditions: (a) the support region is  $-1 < x < 1$ , (b) the first moment of the GPD must be 1 (normalization) for any value of  $/xi$ , (c) in the case of the pion the second moment of the PD must be 1/2 (momentum conservation) and (d) isospin and momentum conservation imply that the PD of the pion must be symmetric under the change  $x \rightarrow (1-x)$ . As to condition (a), the pion vertex function in our model is expressed in Minkowski spacetime and has an intricate analytic structure as opposed to Ref. [29]. It was already argued in our previous work [18] that this can lead to a support problem. Condition (b) is theoretically fulfilled in our model and has been checked numerically [27]. Condition (c) is not fulfilled in our model and may be attributed

to large off-shell effects. Concerning condition (d), isospin symmetry translates into condition (7) in our model, and this has been confirmed numerically to be valid for every value of  $\xi$  and  $t$ .

## 5 Results and Discussion

The  $\pi^+$  up-quark GPD results in the three different model variants are shown in figs. 4 - 6, the  $K^+$  up-quark and strange-antiquark GPDs in figs. 7 - 8. A three-dimensional picture of the (full model)  $\pi^+$  up-quark GPD as a function of  $x$  and  $t$  with skewedness  $\xi = 0$  is presented in fig. 9. For all cases, the results are shown for a representative selection of  $t$  and  $\xi$  values.

It was shown in ref. [18] that GPDs in the Bonn Model violate the support condition. This can also be deduced from figs. 4 - 8. In general, the curves tend to have longer

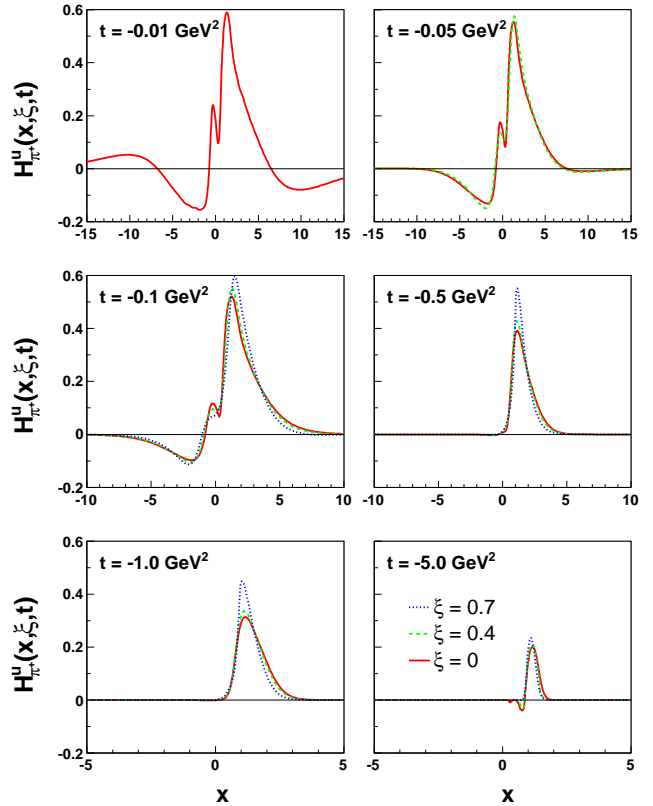


**Fig. 4.** The pion GPD  $H_{\pi^+}^u$  in the full model for different values of  $t$ . Values for  $\xi$  shown are  $\xi = 0$  (red, solid line),  $\xi = 0.4$  (green, dashed line) and  $\xi = 0.7$  (blue, dotted line).

tails as  $|t|$  decreases. Especially for the deeply bound pion in the full model, this effect is clearly visible (see fig. 9). As the relative binding energy decreases, the effect becomes smaller. Furthermore, whereas the maximum of the GPD curve lies outside the support region for the deeply bound

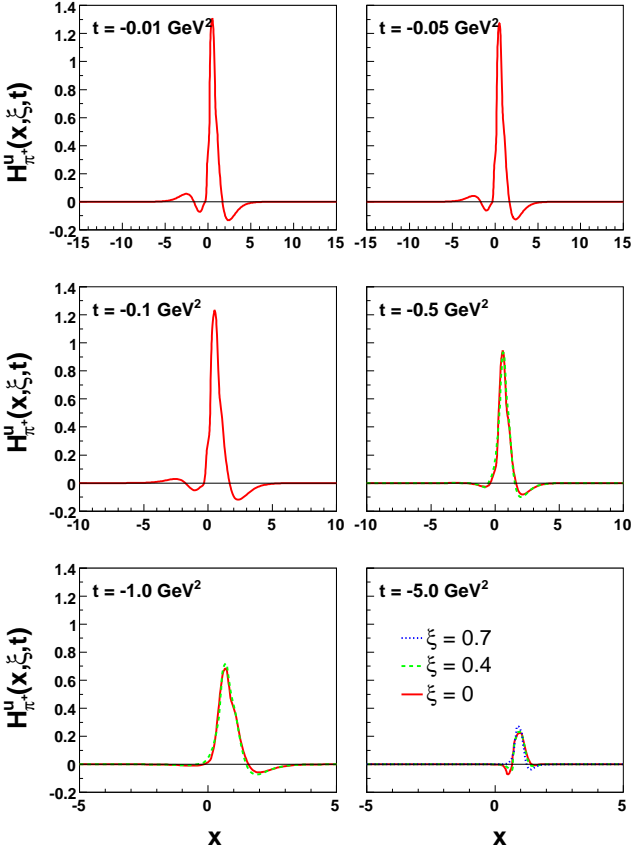


**Fig. 5.** The pion GPD  $H_{\pi^+}^u$  in the reduced model for different values of  $t$ . Values for  $\xi$  shown are  $\xi = 0$  (red, solid line),  $\xi = 0.4$  (green, dashed line) and  $\xi = 0.7$  (blue, dotted line).

pion in the full model (peak value at  $|x| > 1$ ), it lies within the support interval for the other pion and kaon calculations.

Another observation which can be made, is that the pion GPD in the full model displays a clear shoulder in the region  $x \in [0, 1]$  at  $|t| \lesssim 0.1 \text{ GeV}^2$  (see fig. 4). This shoulder is much less pronounced or even absent in the other results. In this respect, it is interesting to note that the computed pion form factor shows a bump at low  $Q^2 = -t$ , which can be ascribed to the instantaneous approximation [11,30,31]. The observed shoulder in the pion GPD might therefore be an artefact of this *Ansatz*.

A direct comparison with other model calculations ([2, 4]) is not straightforward due to the different behavior with respect to the support properties. A double-peaking behavior for  $x = (1 \pm \xi)/2$  in the reduced or IQM model variants is not seen. In both of these models, however, the binding energy represents a significant portion of the meson mass: about 1/3 (1/2) for the reduced (IQM) model (see Table 1). This is in contrast with the calculations of Ref. [2], where the meson mass is very close to the sum of the quark masses and the double-peaking behavior emerges.

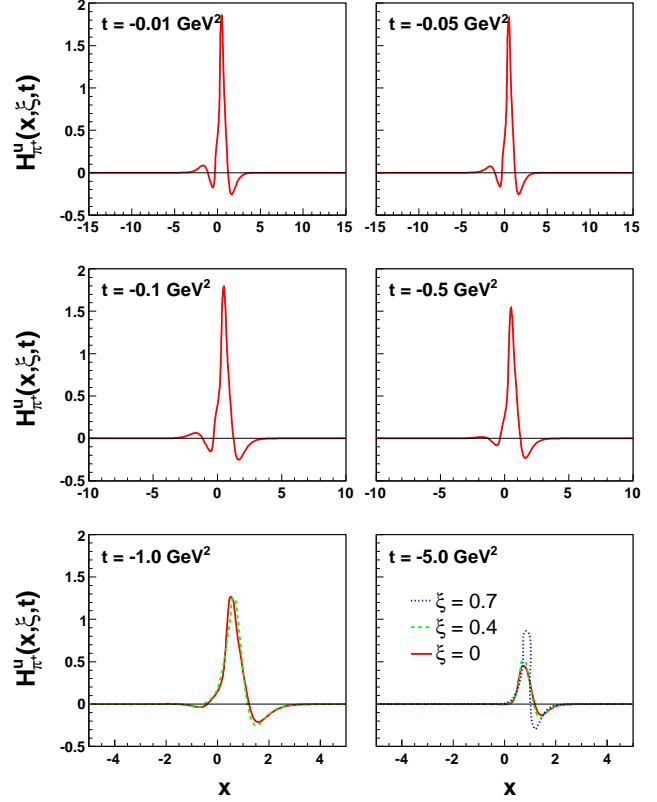


**Fig. 6.** The pion GPD  $H_{\pi^+}^u$  in the IQM model for different values of  $t$ . Values for  $\xi$  shown are  $\xi = 0$  (red, solid line),  $\xi = 0.4$  (green, dashed line) and  $\xi = 0.7$  (blue, dotted line).

The observed model dependence of the GPD properties points at a significant relative binding energy dependence of the support of the generalized parton distributions in the Bonn model. To quantify the support problem, a support parameter ( $\phi$ ) is introduced. For the pion, the generalized quark and antiquark distributions are related via the isospin symmetry relation (7), so that the knowledge of one of them implies the knowledge of the other. The support parameter is therefore defined through the quark GPD:

$$\phi = \frac{\int_{-\xi}^1 |H_{\pi^+}^u(x, \xi, t)| dx}{\int_{-\infty}^{\infty} |H_{\pi^+}^u(x, \xi, t)| dx}. \quad (26)$$

$\phi$  is a measure for the relative support violation: when the correct kinematical regions are resolved,  $\phi = 1$ . The smaller  $\phi$ , the worse the support. For the kaon, the isospin symmetry relation (7) is not valid and different support parameters are introduced for the quark and antiquark GPDs:

$$\phi^q = \frac{\int_{-\xi}^1 |H_{K^+}^u(x, \xi, t)| dx}{\int_{-\infty}^{\infty} |H_{K^+}^u(x, \xi, t)| dx} \quad (27)$$

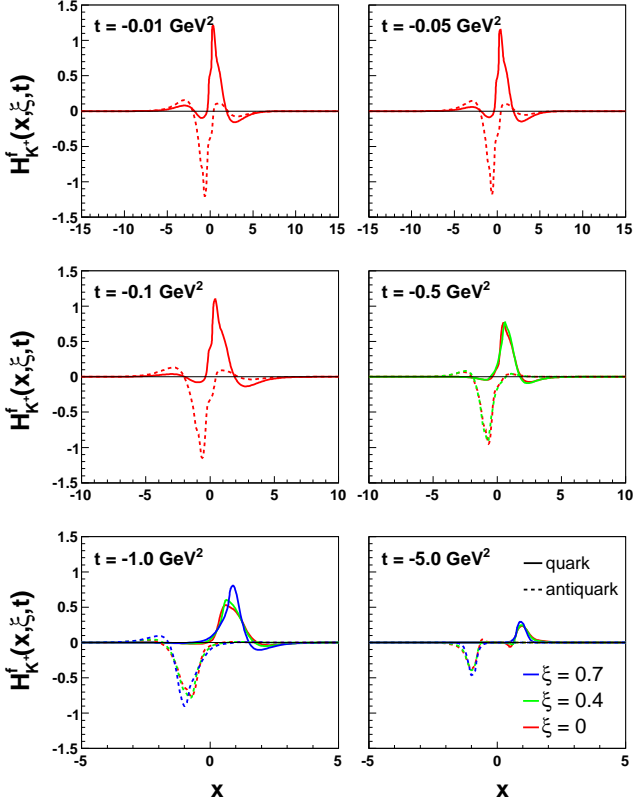


**Fig. 7.** The kaon GPDs  $H_{K^+}^u$  and  $H_{K^+}^s$  in the full model for different values of  $t$ . Values for  $\xi$  shown are  $\xi = 0$  (red line),  $\xi = 0.4$  (green line) and  $\xi = 0.7$  (blue line). The solid line refers to the  $u$  GPD, the dashed line to the  $\bar{s}$  GPD.

and

$$\phi^{\bar{q}} = \frac{\int_{-1}^{\xi} |H_{K^+}^s(x, \xi, t)| dx}{\int_{-\infty}^{\infty} |H_{K^+}^s(x, \xi, t)| dx}. \quad (28)$$

The difference between  $\phi^q$  and  $\phi^{\bar{q}}$  will be used to investigate the flavor dependence of the support problem.

Table 2 lists the values of the support parameter  $\phi$  for the pion GPD results of figs. 4 - 6. Table 3 shows the values of the parameters  $\phi^q$  and  $\phi^{\bar{q}}$  belonging to the kaon curves of figs. 7 and 8.

For the pion GPD, it is seen from table 2 that the support is much better in the reduced and the IQM models than in the full model. In going from the full model to either of the two other models in which the pion is less deeply bound, the support parameter increases significantly (*e.g.* from 0.08 in the full model to 0.60 in the reduced and 0.66 in the IQM model for  $t = -0.01 \text{ GeV}^2$  and  $\xi = 0$ ). We observed in the previous paragraph that, especially for the pion in the full model, the GPD curves tend to broaden with decreasing  $|t|$ . Table 2 shows that this behavior can be attributed to the support properties of the curves. For fixed skewedness  $\xi$ , the support improves for increasing  $|t|$  except for very large values ( $|t| \gtrsim 5.0 \text{ GeV}^2$ ). For a fixed  $|t|$ , the  $\phi$  exhibits hardly any dependence on  $\xi$ .

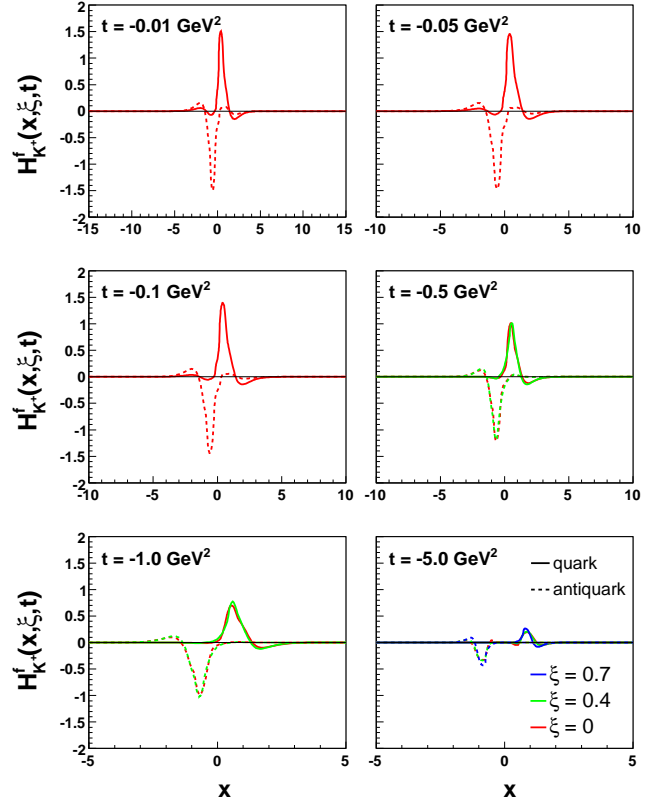


**Fig. 8.** The kaon GPDs  $H_{K^+}^u$  and  $H_{K^+}^s$  in the reduced model for different values of  $t$ . Values for  $\xi$  shown are  $\xi = 0$  (red line),  $\xi = 0.4$  (green line) and  $\xi = 0.7$  (blue line). The solid line refers to the  $u$  GPD, the dashed line to the  $\bar{s}$  GPD.

Also for the kaon GPD, the support improves when the instanton induced interaction is switched off. Notice that the values of the two support parameters  $\phi^q$  and  $\phi^{\bar{q}}$  are similar. This result is compatible with the finding that the quark and antiquark GPD have similar shapes and shows that the small differences between both GPDs do not alter the support significantly. Combining these observations with the fact that the support does improve significantly in the IQM model with respect to the full model, we conclude that concerning the support the binding strength is more important than the particular constituent quark mass or flavor.

## 6 Summary and Conclusions

In this work, the isoscalar twist-two generalized parton distributions of the pion and the kaon were calculated in the Poincaré covariant Bethe-Salpeter constituent quark model developed by the Bonn group. The first moment of the GPD in the full  $x$ -region equals the electromagnetic form factor. Results were shown in the full  $x$ -region for several values of  $\xi$  and  $t$ . It turns out that the Bonn model violates the support condition. We have illustrated



Model	$\xi$	$t$ (GeV <sup>2</sup> )					
		-0.01	-0.05	-0.1	-0.5	-1.0	-5.0
Full model	0	0.08	0.11	0.13	0.21	0.20	0.17
	0.4	-	0.12	0.14	0.21	0.22	0.17
	0.7	-	-	0.12	0.17	0.20	0.12
Reduced model	0	0.60	0.62	0.64	0.69	0.69	0.63
	0.4	-	-	-	0.70	0.71	0.61
	0.7	-	-	-	-	-	0.56
IQM model	0	0.66	0.67	0.67	0.71	0.73	0.68
	0.4	-	-	-	-	0.75	0.70
	0.7	-	-	-	-	-	0.64

**Table 2.** Values of the pion support parameter  $\phi$  of eq. (26) corresponding to figs. 4 - 6.

Parameter	Model	$\xi$	$t$ (GeV <sup>2</sup> )					
			-0.01	-0.05	-0.1	-0.5	-1.0	-5.0
$\phi^q$	Full model	0	0.46	0.48	0.50	0.58	0.61	0.47
		0.4	-	-	-	0.60	0.62	0.48
		0.7	-	-	-	-	0.56	0.56
	Reduced model	0	0.68	0.69	0.70	0.73	0.73	0.64
		0.4	-	-	-	0.76	0.75	0.62
		0.7	-	-	-	-	-	0.63
$\phi^{\bar{q}}$	Full model	0	0.43	0.45	0.47	0.56	0.61	0.42
		0.4	-	-	-	0.58	0.61	0.43
		0.7	-	-	-	-	0.55	0.57
	Reduced model	0	0.65	0.66	0.67	0.72	0.73	0.65
		0.4	-	-	-	0.73	0.74	0.64
		0.7	-	-	-	-	-	0.69

**Table 3.** Values of the kaon quark and antiquark support parameters of eq. (28) corresponding to figs. 7 - 8.

the strong correlation between the support and the (relative) binding energy of the meson. Therefore, the deep binding of the pion induces strong support violations. We have found that  $\xi$  hardly influences the support, whereas a moderate dependence on  $t$  is predicted. The constituent quark masses have an impact on the support, but only through the (relative) binding energy. A mass difference between constituent quarks hardly affects the corresponding GPD curves.

The reason for the violation of the support condition in the Bonn constituent quark model is not fully understood: It might be related to the instantaneous approximation made. Although this assumption is formally covariant, the neglect of retardation effects could lead to wrong analytic properties of the hadronic vertex functions, in particular for “deeply-bound” states such as the pion. Some hints in this direction were already found earlier in the calculated pion electromagnetic form factor, which showed a conspicuous unphysical structure at small momentum transfers [30,31]. The present detailed analysis provides additional support for this conjecture.

The observed support properties of the Bonn constituent quark model could also be interpreted as follows. As the Bonn model is a *soft scale* model, with neither on-shell particles nor asymptotic freedom properties, the support violation can be considered as a manifestation of soft scale physics. This prohibits the use of the available QCD-based

evolution equations to the model. In contrast, a soft-scale model with the correct support properties can be evolved. It should be clear, however, that also in this case, the use of the evolution equations relies on an extrapolation of perturbative QCD to soft scales. Additionally, it should be noted that the Mellin moments of the GPDs at  $\xi = 0$  can be evolved, even in the case of a support violation.

### Acknowledgements

The authors wish to thank F. Llanes Estrada, S. Scopetta and D. Van Neck for enlightening discussions. AVD and TVC are grateful to the Research Foundation - Flanders (FWO) for financial support. BCM acknowledges the support of the European Community-Research Infrastructure activity under the FP6 “Structuring the European Research Area” programme (Hadron Physics, contract number RII3-CT-2004-506078) and the support within the DFG SFB/TR16 “Subnuclear Structure of Matter - Elektromagnetische Anregung subnuklearer Systeme”.

### References

1. S. Boffi, B. Pasquini, arXiv:0711.2625 [hep-ph] (2007)
2. S. Noguera, L. Theußl, V. Vento, Eur. Phys. J. **A20**, 483 (2004)

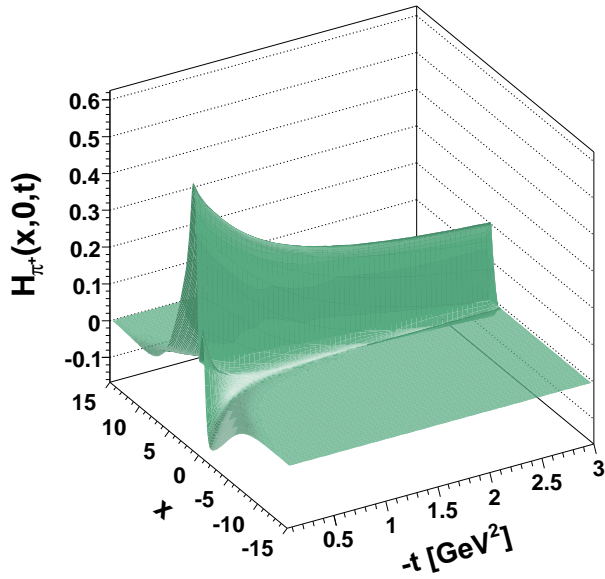


**Fig. 9.** The  $H_{\pi^+}^u(x, 0, t)$  GPD in the full model as a function of  $x$  and  $-t$  for  $\xi = 0$ .

3. F. Bissey, J. Cudell, J. Cugnon, J. Lansberg, P. Stassart, Phys.Lett. **B587**, 189 (2004), [hep-ph/0310184](#)
4. B. Tiburzi, G. Miller, Phys. Rev. **D65**, 074009 (2002)
5. B. Tiburzi, G. Miller, Phys. Rev. **D67**, 054014 (2003)
6. B. Tiburzi, G. Miller, Phys. Rev. **D67**, 054015 (2003)
7. L. Kisslinger, H.M. Choi, C.R. Ji, Phys. Rev. **D63**, 113005 (2001)
8. H.M. Choi, C.R. Ji, L. Kisslinger, Phys. Rev. **D64**, 093006 (2001)
9. H.M. Choi, C.R. Ji, L. Kisslinger, Phys. Rev. **D66**, 053011 (2002)
10. A. Van Dyck, T. Van Cauteren, J. Ryckebusch, B. Metsch, H.R. Petry, Prog. Part. Nucl. Phys. **61**(1), 175 (2008)
11. M. Koll, R. Ricken, D. Merten, B.C. Metsch, H.R. Petry, Eur. Phys. J. **A9**, 73 (2000)
12. J. Resag, C.R. Münz, B.C. Metsch, H.R. Petry, Nucl. Phys. **A578**, 397 (1994)
13. C.R. Münz, J. Resag, B.C. Metsch, H.R. Petry, Nucl. Phys. **A578**, 418 (1994)
14. C.R. Münz, Ph.D. thesis, Rheinische Friedrich-Wilhelms-Universität Bonn, Germany (1994), [http://www.itkp.uni-bonn.de/publications/bspub.html](#)
15. R. Jaffe, Phys. Lett. B **93**, 313 (1980)
16. M. Diehl, Phys. Rept. **388**, 41 (2003), [hep-ph/0307382](#)
17. R. Jaffe, Nucl. Phys. **B229**, 205 (1983)
18. A. Van Dyck, T. Van Cauteren, J. Ryckebusch, Phys. Lett. B **662**, 413 (2008), [arXiv:0710.2271](#)
19. X. Ji, J. Phys. **G24**, 11811 (1998), [hep-ph/9807358](#)
20. A. Radyushkin, Phys. Rev. **D56**, 5524 (1997), [hep-ph/9704207](#)
21. X. Ji, Phys. Rev. Lett. **78**, 610 (1997)
22. B.C. Metsch, H.R. Petry, Acta Phys. Polon. **B27**, 3307 (1996)
23. E.E. Salpeter, H.A. Bethe, Physical Review **84**, 1232 (1951)
24. E.E. Salpeter, Phys. Rev. **87**, 328 (1952)
25. G. 't Hooft, Phys. Rev. **D14**(12), 3432 (1976)
26. R. Ricken, Ph.D. thesis, Rheinische Friedrich-Wilhelms-Universität Bonn, Germany (2001), [http://www.itkp.uni-bonn.de/publications/bspub.html](#)
27. A. Van Dyck, Ph.D. thesis, Universiteit Gent (2008), [http://inwpent5.ugent.be/papers/phdannelies.pdf](#)
28. S. Mandelstam, Proc. Roy. Soc. **233**, 248 (1955)
29. S. Noguera, V. Vento, Eur. Phys. J. **A28**, 227 (2006)
30. M. Koll, Ph.D. thesis, Rheinische Friedrich-Wilhelms-Universität Bonn, Germany (2001)
31. C.R. Münz, J. Resag, B.C. Metsch, H.R. Petry, Phys. Rev. **C52**(4), 2110 (1995)